ASTM A743-CA6NM Surface Modification with Fe-Mn-Cr-Si Cavitation Resistance Alloy

Anderson Geraldo Marenda Pukasiewicz, anderson @utfpr.edu.br
Fernando Ratti de Oliveira, fernando_piu@hotmail.com
UTFPR Universidade Tecnológica Federal do Paraná - Campus Ponta Grossa,
Av. Monteiro Lobato s/n, km04, Ponta Grossa, Paraná, Brasil, CEP 84016-210

André Ricardo Capra, andre.capra@lactec.org.br
LACTEC, Instituto de Tecnologia para o Desenvolvimento,
Av. Lothário Meissner, nº01, Jardim Botânico, Curitiba, Paraná, Brasil, CEP 80210-170

Ramón Sigifredo Cortés Paredes
UFPR, Universidade Federal do Paraná,
Rua Francisco H. dos Santos, s/n, Curitiba, Paraná, Brasil, CEP81531-980

Abstract. *ASTM A743-CA6NM is a modification of CA15 steel that have been used in hydraulic turbines, but still it shown restrictions with reference to the welding recovery of eroded areas. GMAW welding is the most common technique used to recover geometrical profile of cavited blades. However it is known that tensile residual stress can be occurs. Development of manufacture process, that could reduce or eliminate the residual stress level, will contribute for a longer service life of this component. Cavitation resistance coatings deposition in turbine blades is another important way to increase the service life oh these components. Fe-Cr-Mn-Si is a cavitation resistance class of steel with high induced strain hardening by phase transformation and lower stacking fault energy. The purpose of this work is to evaluate the metallurgy of ASTM A743-CA6NM surface modification with Fe-Mn-Cr-Si deposited by arc thermal spray process and plasma remelting. Different levels of conventional and pulsed current of plasma transferred arc were evaluated. Base metal dilution, microhardness, chemical composition, as well as HAZ microhardness and length were analyzed. Microstructure of the coating and HAZ were evaluated by optical and electronic microscopy. Arc thermally sprayed coatings showed 1,02±0,91% of porosity and 18,24±4,98% of area fraction oxide. Good weldability without crack and low porosity content were observed in all remelted coatings. The increase in arc current promotes a dilution increase of the coating. Fe-Mn-Cr-Si remelted coating presents austenite and martensite phase with decreasing in microhardness from 328,7Hv to 296,2Hv with pulsed arc current increase from 100/80A to 180/80A. Arc thermally sprayed remelted coatings showed to be a good alternative for deposition of cavitation resistance materials on soft martensitic stainless steel eroded areas.*

Keywords*: cavitation, surface alloying, soft martensitic stainless steel*

1. INTRODUCTION

The process of cavitation mass loss is one of the main problems that occurs in maintenance of turbine hydraulic runners (Huth, 2005). This problem is caused when a surface is exposed to a fluid with a localized pressure reduction, which promotes the formation of bubbles. When these bubbles move to a higher pressure area, vapor or gas bubbles collapse with a great energy release on the surface, causing mass loss. Cavitation erosion is frequently found in operation of hydraulic equipments as: hydropower turbines, valves, pumps and ships propellants (March and Hubble, 1996).

Stainless steels are one of the most filler material used in cavitation repair. AWS ER309LSi is one of the most used alloys, because of its good weldability, adequate cavitation resistance and low cost. Stainless steel alloys with cobalt commercially known as Cavitec and Cavitalloy present better cavitation behavior compared to common stainless steel. These alloys presents low stacking-fault energy, SFE, and strain induced martensite transformation (Simoneau, 1987 and 1991).

Many works have correlated high cavitation resistance with different metallurgic properties, as deformation hardening, strain induced transformation, low SFE, cyclic strain hardening and fatigue resistance, with better correlation with low SFE (Richman, 1990, Simoneau, 1987 and 1991).

Fe-Mn-Cr-Si alloys are kind of alloys with shape memory capacity, that occurs by their low SFE and strain induced martensite transformation (Otuka, et al, 1990, Matsumura, et al, 2000). These properties and the good results with NiTi shape memory alloys (Cui, et al, 2003, Chiu, et al., 2005, Stella, et al. 2006), encouraged the use of these alloys in cavitation resistance materials and coatings (Wang, Z., Zhu, J., 2003 and 2004, Pukasiewicz, 2008).

Nowadays hydraulic turbine runners are normally manufactured with soft martensitic stainless steels containing 12–13% chrome, 2–5% nickel and less than 0.06% carbon (Bilmes, et al, 2000 and 2001). This steel is a modification of CA15 which contains higher levels of carbon and consequently a harder martensite (Folkhard, 1988). High yielding

stress and tenacity, high cavitation resistance and good weldability are properties of these stainless steels. Martensitic steels with low carbon content, such as CA6NM steel, are always quenched and tempered.

The excellent tenacity of these steels occurs by fine dispersion of austenite on martensite, during tempering treatment at temperatures in the order of 600 ºC. Beside austenite precipitation, low carbon content promote a formation of a soft martensite with tenacity increase, rising hydrogen-induced cracking resistance, compared with standard martensitic grades (Lippold and Kotecki, 2005).

Although this class of steel shown a softer martensite formation, good weldability and less demanding requirements with regard to pre-heating and interpass temperatures, the weld metal (WM) and the heat affected zone (HAZ) have lower impact energy than observed in base metal (BM) (Akhtar and Brodie, 1979).

Eroded cavitated areas in hydraulic turbine runners are recovery mainly with GMAW (gas metal arc welding) with austenitic stainless steel or alloys with more resistance with cobalt and manganese addition. However GMAW presents some limitations, like high residual stress and sometimes low tenacity mainly in martensitic stainless steel even in low carbon alloys (Musardo, *et al.*, 2005). High residual stresses occurs due thermal cycles caused by the heating and solidification contraction of the weld pool that reduce the service life of these components (Arai, et al, 1995, Boy, et al, 1997)

With the purpose residual stresses reduction, caused during welding deposition, thermal spraying deposition has been studied to protect hydraulic turbine against cavitation erosion. The main purpose is promote coatings with adequate cavitation resistance without compromising the integrity of the equipment (Kreye, et al, 1998 and March, et al, 1996).

Arc thermal spraying, ASP, is a process that promote the deposition of a metallic material finely divided in a prepared surface to form a protective superficial layer. However, in severe cavitation situations, the ASP thermal spraying presents limited cavitation resistance. This occurs due its microstructure formed by interlamellae oxides and present fragile cracking, causing mass loss (Kreye at al, 1998). With the purpose of eliminate the interlamellae oxide and pores influence, many techniques of remelting have been applied to modify the deposited layer, such as oxyacetylene flame and laser (Chiu, et al., 2005, Gireń, et al., 2005, Mitelea *et al.* 2010 and Kwok, Man, Cheng, 2001).

In this work, the remelting technique employed was plasma-transferred arc, PTA. In this work the main objective is evaluate the influence of continuous current and peak current in pulsed arc in microhardness, chemical composition of the coating, as well as HAZ microhardness and length of CA6NM base metal.

2. EXPERIMENTAL PROCEDURES

The material used was a soft martensitic stainless steel, CA6NM, 1050ºC air quenched and 580ºC tempered, supplied by Voith Siemens company. The material was machined with 243x75x50mm (LxWxH). Chemical compositions of the CA6NM steel and Fe-Mn-Cr-Si 1,26mm wire are presented, Tab. 1.

Table 1. Chemical composition of materials.

	ϕ (mm)	C (wt%)	N (wt%)	Si (wt%)	Mn (wt%)	Cr (wt%)	Ni (wt%)	Mo (wt%)	P (wt%)	S (wt%)
CA6NM		0,02	0,0	0,0	0,64	12,4	3,7	0,42	0,008	0,0018
Fe-Mn-Cr-Si alloy	1,6	0,15	0,20	4,5	20,0	8,0	0,0	0,0	0,0	0,0

Arc spray wire is a metal cored wire that was prepared with low-C steel strip with powder alloying elements addition in a 1,6mm wire. Before coating deposition, samples were machined to final dimensions 25x75x50mm (LxWxH). Followed by abrasive blasting with intend to obtain a clear surface without oxides and impurities. To guarantee better adherence, abrasive blasting parameters are observed in Table 2.

Table 2. Abrasive blasting parameters.

Parameter	
Abrasive	white aluminium oxide #36mesh
Method	Air pressure impingement
Air pressure	80-90psi
Blasting distance	120-150mm
Minimal Rugosity	4,0µm Ra

For spray deposition an eletric arc Suzler-Metco equipment model Value Arc 300E was used in DC mode, with Suzler-Metco Eletric LCAG arc gun and "fine" air cap. Spray deposition was conduced in a normal angle to surface,

90º, with intend to reduce splashing droplets formation to get better adhesion. Arc spray parameters for deposition are listed in Table 3.

Table 3. Coating deposition parameters.

Parameter	
Current (A)	180
Voltage (V)	30
Air Pressure (KPa)	410
Transport gas	Ar-comprimido
Stand-off distance (mm)	120
Coating thickness (µm)	1000±100

Plasma remelting process was realized with PTA (plasma transferred arc) equipment in an IMC450 welding machine with Thermal Dynamics 300 plasma torch. To intend a constant deslocation a Bug'O drive torch system was used. Plasma transferred arc was used because it's high energy density can reduce base metal dilution, parameters used in this research are listed in Table 4.

Table 4. Fe-MnCr-Si plasma remelting parameters.

Current (A)	**Average Current (A)**	**T_p/T_b (s)**	**NPD* (mm)**	**Electrode distance (mm)**	**Plasma gas**	**Protection gas**	**Plasma gas flow (l/min)**	**Protection gas flow (l/min)**	**Remelting velocity (cm/min)**
180-80	130	0,1/0,1	7,0	0,8	Ar	Ar3%CO_2	1,1	12,0	10,0
140-80	110	0,1/0,1	7,0	0,8	Ar	Ar3%CO_2	1,1	12,0	10,0
100-80	90	0,1/0,1	7,0	0,8	Ar	Ar3%CO_2	1,1	12,0	10,0
130	130	-	7,0	0,8	Ar	Ar3%CO_2	1,1	12,0	10,0

* nozzle piece distance

After visual and liquid penetrant inspection, ASP coated and plasma remelted samples were prepared for metallographic characterization with Buehler Isomet 4000 precision saw. Grinding and polishing were realized by Buehler Vector semi-automatic system; 220, 320, 400, 600 and 1200 mesh silicon carbide grinding paper for grinding, and 3,0µm, 0,25µm monocrystalline diamond paste and 0,04µm silical colloidal were used for polishing during metallographic preparation. For microstructure revelation Vilella's etching was used in this work.

Characterization was carried out by optical microscopy in a Olympus BX60 microscope, with acquisition of images through image software analysis, Analysis 5.1. Electronic microscopy was carried out by a Philips microscope model XL30 with EDX analysis for chemical composition measurements. Mechanical property was measured by microhardness Vickers test with 300gf.

3. RESULTS AND DISCUSSION

3.1. Visual Inspection and Macrographs

ASP coated surface is visualized in Fig. 1(a), showing a rough surface, characteristic from a thermal spray process. After PTA remelting, scales formations from solidification are visualized, containing depressions and porosities. These depressions, observed in Fig. 1(b), occurred due oxide removal and flotation from ASP coating, and because fluid flow in weld pool these oxides were deslocated to weld bead side. After liquid penetrant inspection, Fig. 1(c) and (d), porosity formation can be observed in all samples. It was observed an increase in porosity with arc current increase.

Coating thickness is observed in Fig. 2(a), microstructure of Fe-Mn-Cr-Si ASP coating is observed in Fig. 2 (b), ASP microstructure is composed by pores, black areas, oxides formed during the deposition process, dark gray areas and the metallic phase, light gray areas. After etching, Fig. 3, general microstructure (a), and the grain of the metallic phase microstructure, (b), is observed in ASP coating.

In Figure 3 (b) it can be observed that the grain growing showed orientation probably by rapid cooling rates observed in ASP process, around $1{,}6 \times 10^5$ºC/s Newbery, *et al*. (2005), which is responsible to microstructure refining in these coatings. Similar microstructure was observed by Newbery and Grant (2006), in plain carbon steel wire. In this work sub-micron grain microstructure were near the bottom surface and near top surface contains larger grains with 1-3µm of grain size, however this grain size variation was not observed in Fe-Mn-Cr-Si coatings.

After ASP deposition, base metal did not shown significant modification in microstructure and microhardness, however some deformation in base metal and micro cracks near blasted surface were observed in arc thermally sprayed samples, Fig. 4.

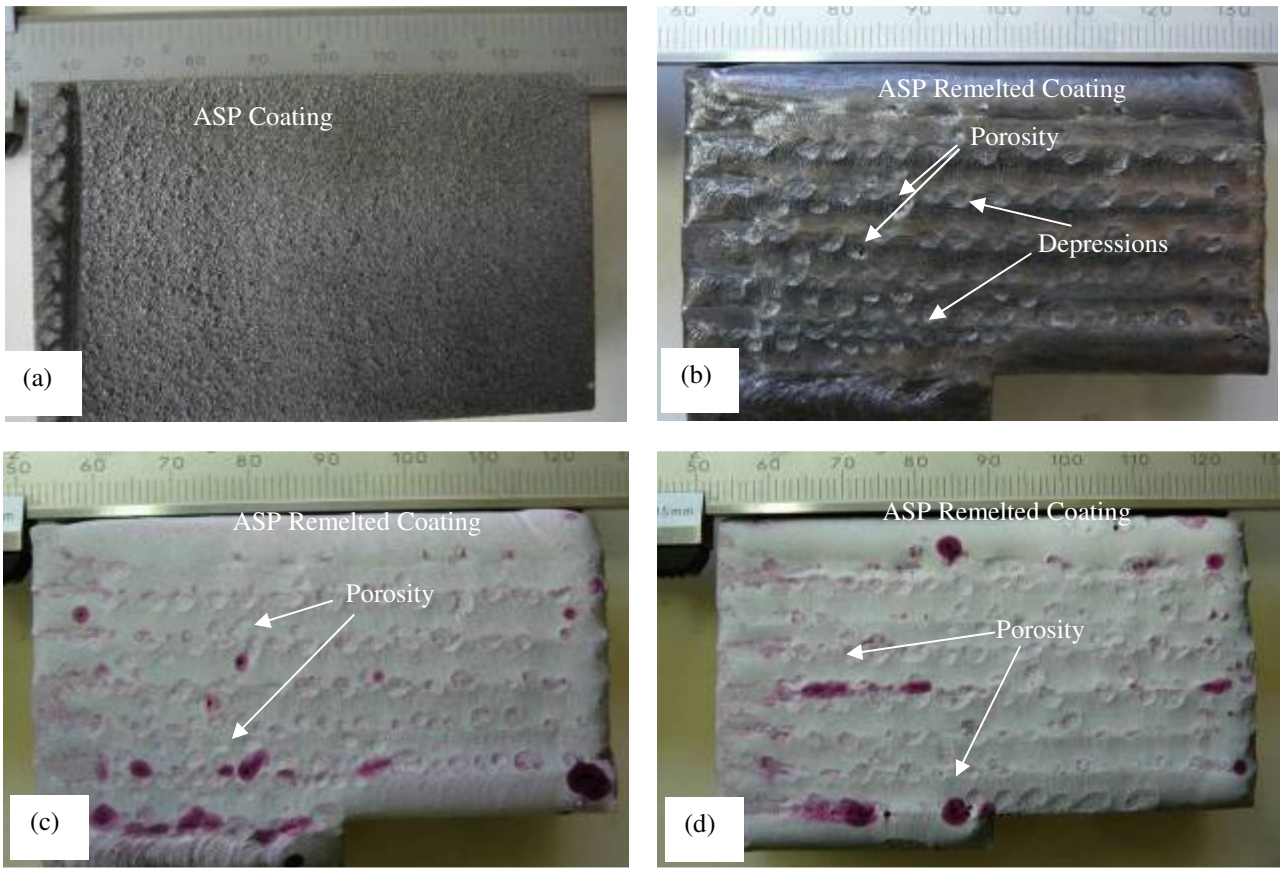

Figure 1. ASP coating before PTA remelting (a) and after remelting (b). Liquid penetrant inspection

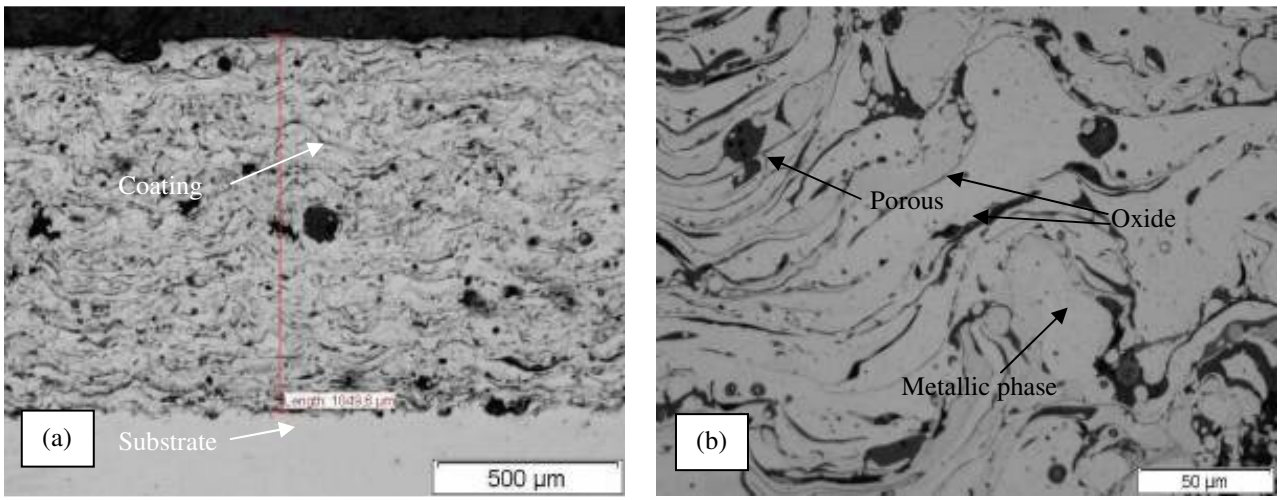

Figure 2. ASP microstructure, (a) coating thickness 100x, (b) pores, oxide and metallic phase formation 500x.

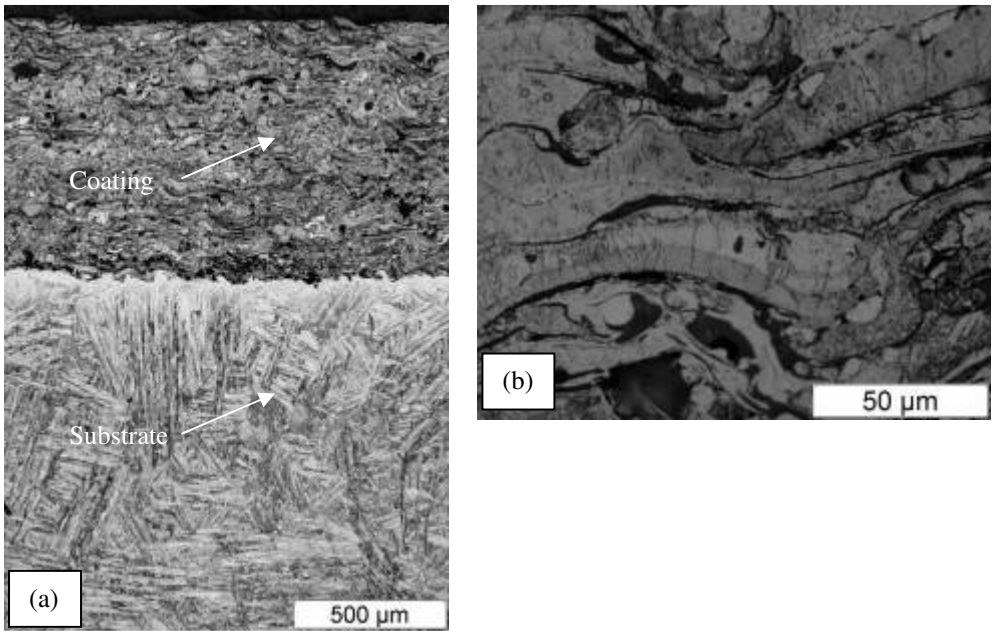

Figure 3. ASP microstructure, (a) general aspect, (b)lamellae grain microstructure.

In remelted microstructure, pores and oxides, present in sprayed coatings, were not observed in the remelted coating, Fig. 5 (a), some areas without remelting can be visualized in Fig. 5 (b), these areas are localized among remelting beads because of overlap failure position during plasma remelting.

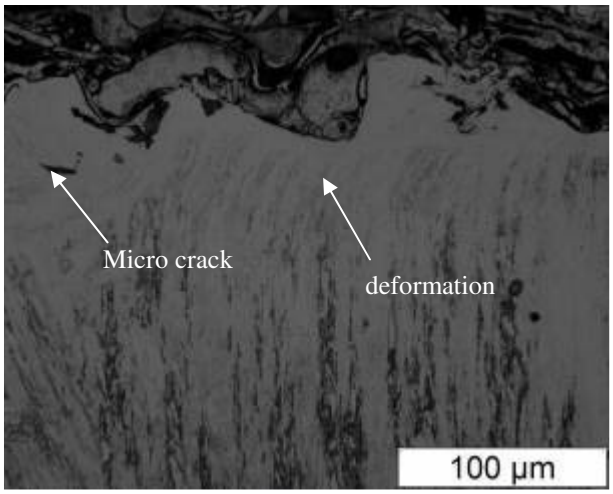

Figure 4. Base microstructure deformation sub-surface micro cracks near blasted surface.

3.2. Microstructure and Microhardness remelted coating evaluation

In Figure 6, Fe-Mn-Cr-Si remelted microstructure can be observed, remelted coatings showed a similar microstructure than welded samples, with oriented dendritic solidification. It can be observed martensitic structure formation in all samples, these martensitic structure formation are more clearly observed inside the dendrite structure. A thin martensite plates indicate that some quantity of martensite is a strain induced martensite formation, Bergeon, *et al*., 1997, due a low stacking fault energy of these alloys, Otsuka *et al*., 1990. This behavior need to be evaluated by XRD (X-ray diffraction) to measure α and ε martensite contents, which can affect the cavitation resistance of the coating.

Solidification grain boundary can be visualized in Fig.6 (f) and (h), solidification subgrain boundary can be visualized in Fig. 6 (d) and (f) with apparent martensite formation inside this cells and dendrites.

In SMA_100/80, Fig 6(e) some unmelted layers between coating and substrate can be visualized, this lower heat input level did not promote a base metal dilution in some areas, therefore plasma remelting did not promote a metallurgic bonding with this energy level with this coating thickness.

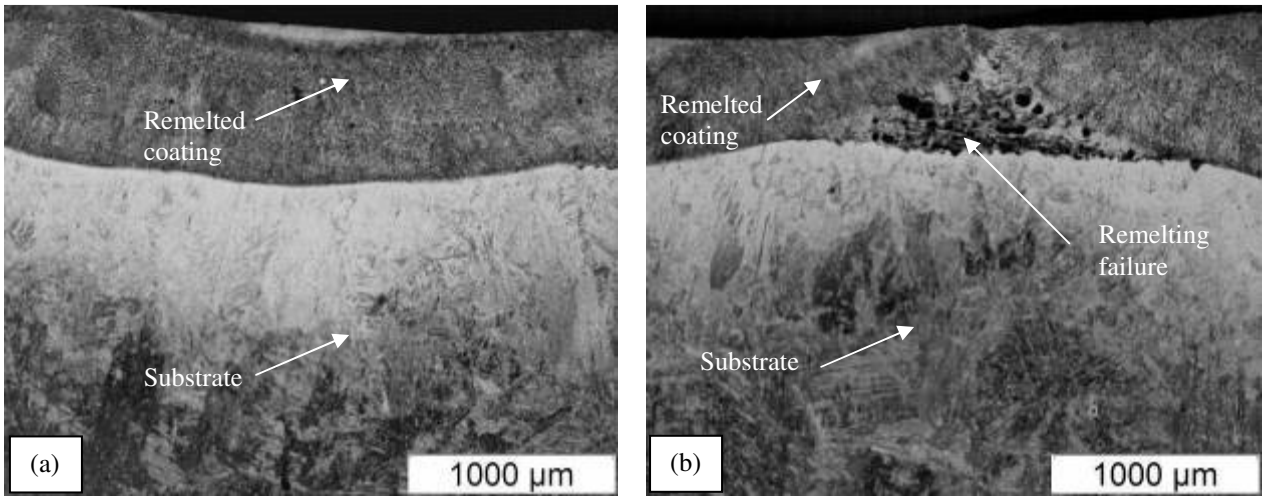

Figure 5. ASP remelted coating layer, SMA_140/80 (a), remelting failures are visible among remelted beads (b).

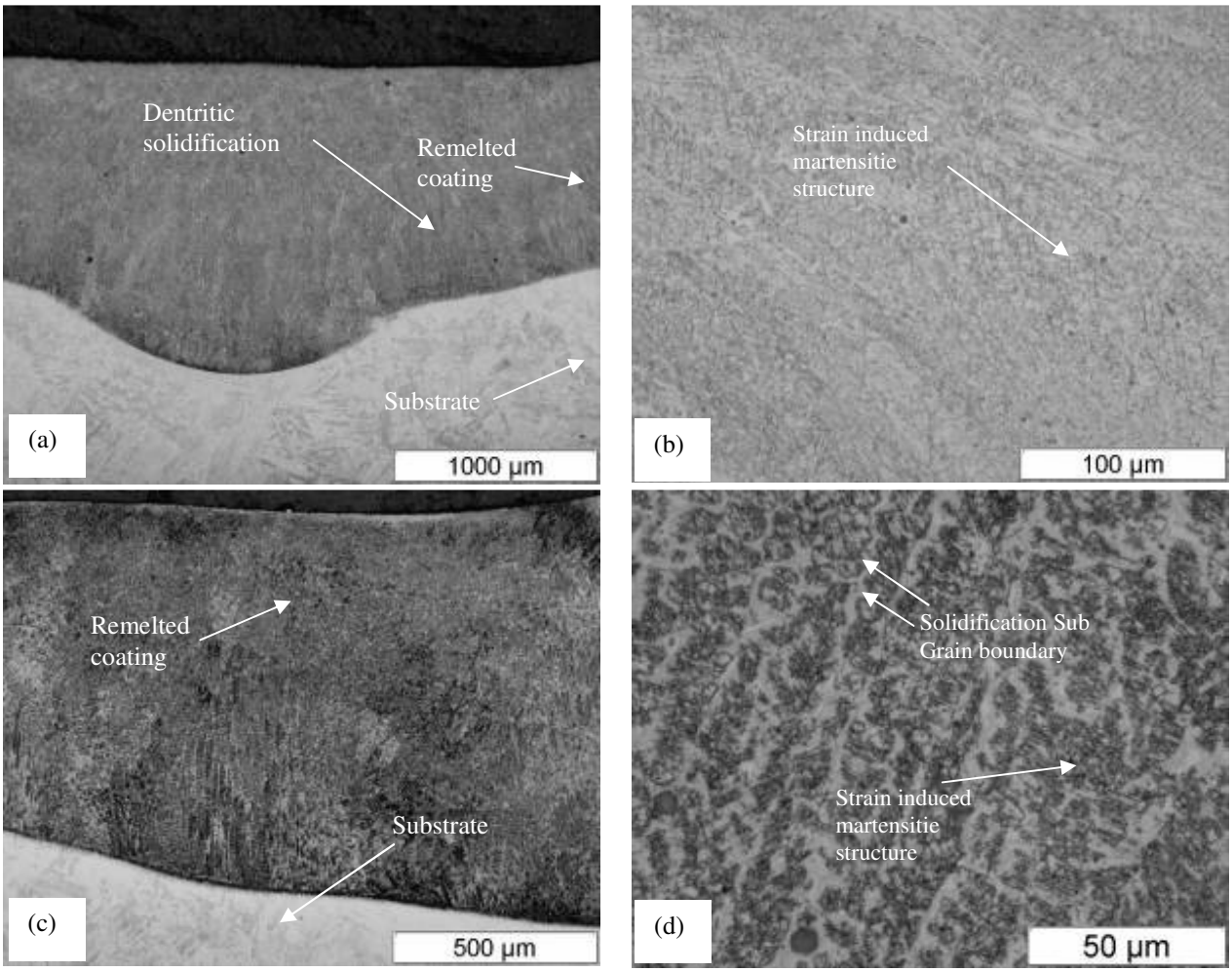

Figure 6. Fe-Mn-Cr-Si remelted microstructure (a,b) SMA_180/80, (c,d) SMA_140/80, (e,f) SMA_100/80, (g,h) SMA_130.

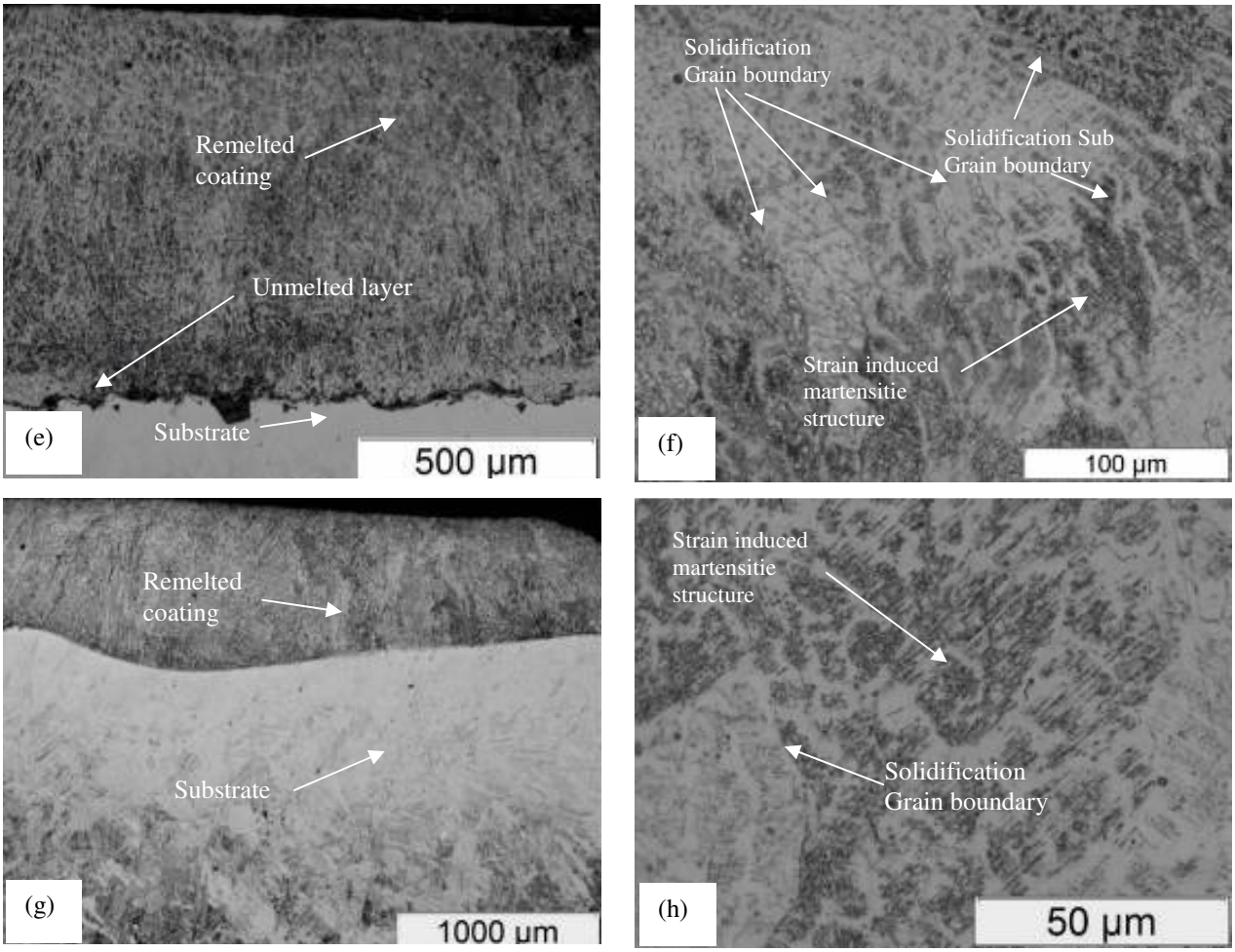

Figure 6 (cont.). Fe-Mn-Cr-Si remelted microstructure (a,b) SMA_180/80, (c,d) SMA_140/80, (e,f) SMA_100/80, (g,h) SMA_130.

Martensite formation, inside dendrite solidification structure, is clearly observed in SEM, Fig. 7, as well as solidification grain boundary and sub-grain boundary. Martensite formation occurs inside solidification subgrains boundary, these martensite formation was verified in optical microscopy observation, Fig. 6 (d) and (f). During solidification solute redistribution causes these boundaries, Lippold and Kotecki, 2005, this solute redistribution probably promotes a preferential martensite formation inside subgrains boundary, however the difference in chemical composition between these two regions did not observed.

In Figure 8 it can be observed Mn and Si reduction with increase in peak current, because these elements are present in major quantity in filler metal than base metal, otherwise, rise in Ni content in samples with higher peak current it was observed.

A slightly difference in Mn and Ni content between samples with same value of average current, SMA_180/80 and SMA_130 was identified, probably because of the differences in melt pool convection by pulsed current use.

Microhardness measurement profile of ASP coating as deposited showed a higher scatter results than remelted coatings, this behavior is expected because of the pores and oxide presence in an inhomogeneous microstructure, Fig. 9. Microhardness of remelted coatings showed slight difference among tested samples with peak current values variation, Fig 9(a) and samples with pulsed and constant current, Fig. 9(b). It was observed a tendency to microhardness decrease with peak current increase and the use of constant arc current did not modify microhardness profile in this work.

CA6NM HAZ microhardness and length rise was observed after PTA remelting process independently of the arc current, in compared with ASP as coated HAZ. It can be observed in Fig 9(a) an decrease in microhardness and HAZ CA6NM length with constant current in compared with pulsed arc current with the same level of heat input.

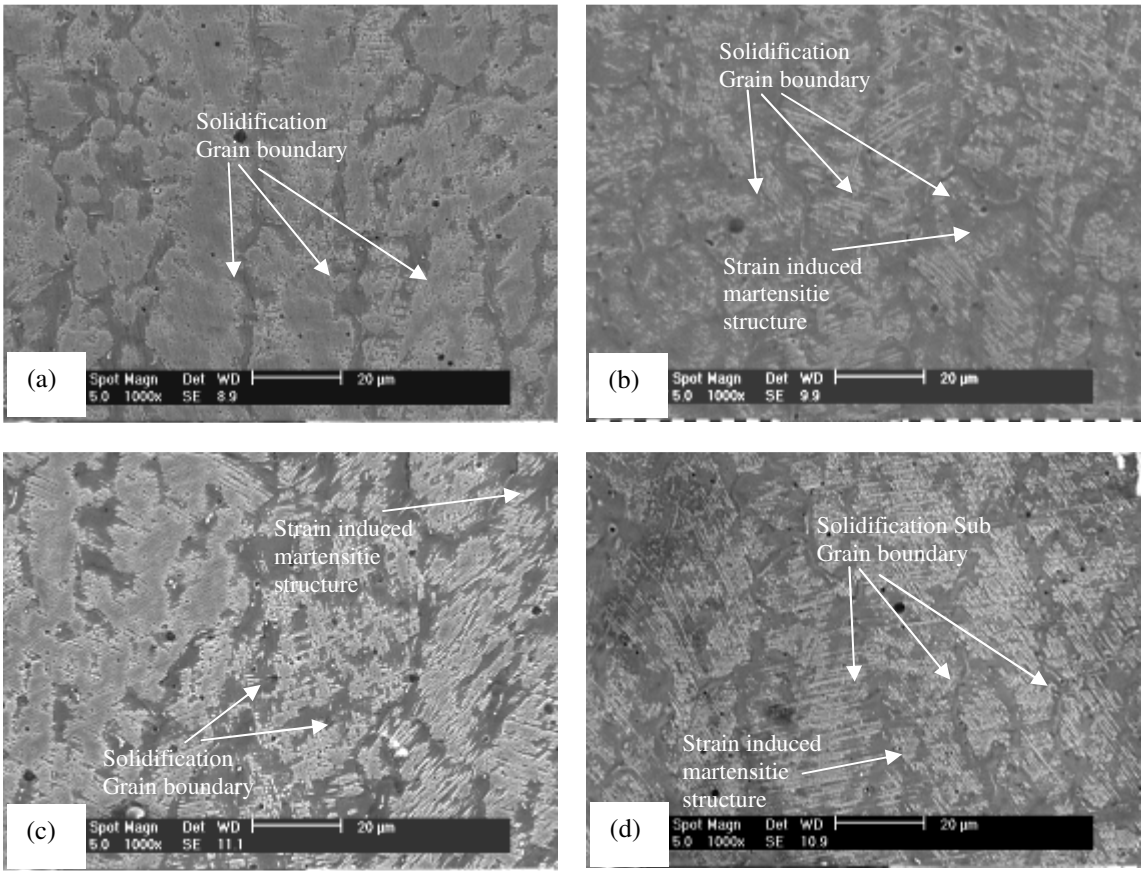

Figure 7. ASP remelted microstructure, SEM (a) SMA_180/80, (b) SMA_140/80, (c) SMA_100/80 and (d) SMA_130.

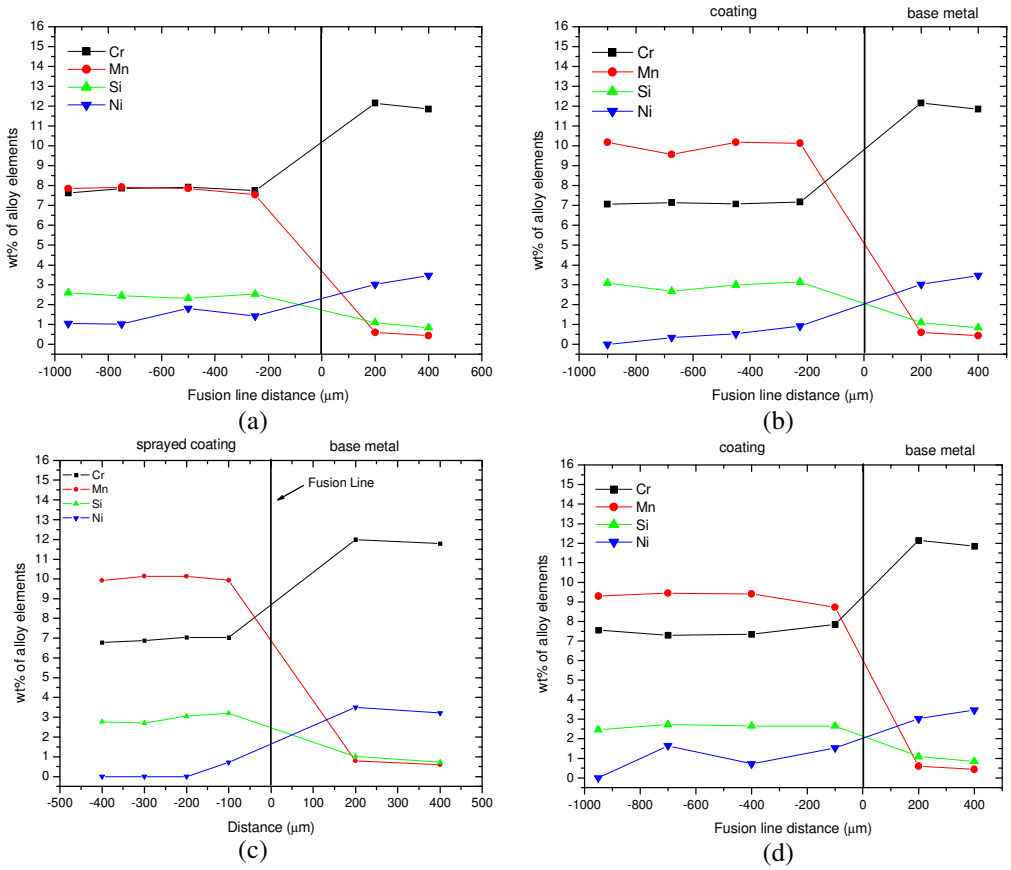

Figure 8. ASP remelted chemical composition (a) SMA_180/80, (b) SMA_140/80, (c) SMA_100/80 and (d) SMA_130.

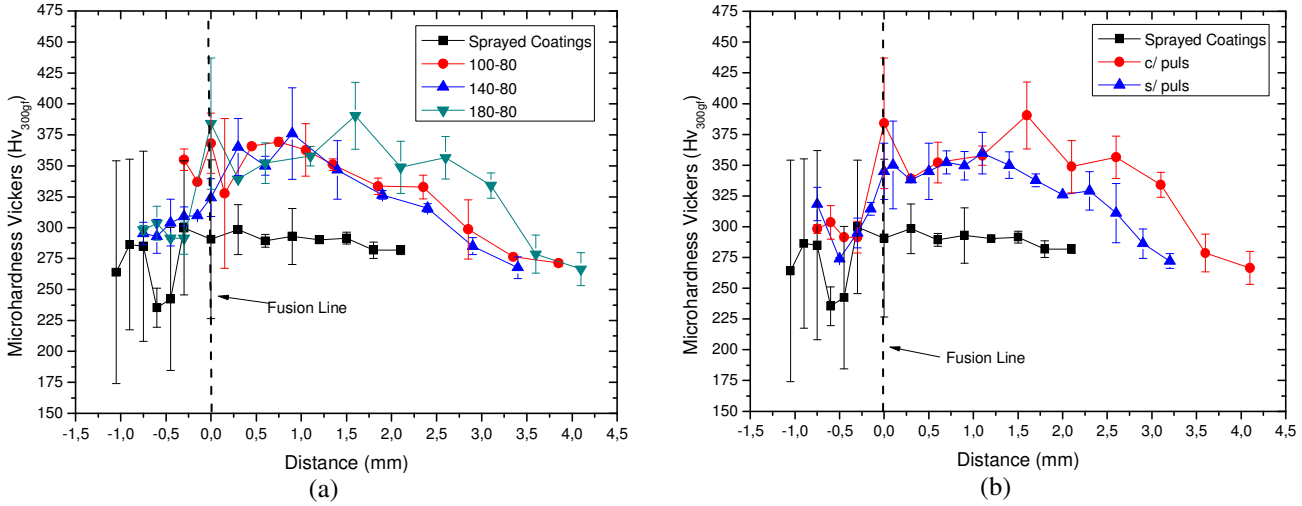

Figure 9. Remelted ASP coatings microhardness profile (a) Different levels of peak current, (b) Pulsed and conventional current.

4. CONCLUSIONS

Remelting process by PTA plasma removes the pores and oxides from the coating, reducing hardness scatter rising coating hardness. Some areas without remelting occured among remelting beads because of overlap failure position during plasma remelting.

It can be observed martensitic structure formation in all remelted samples, these martensitic structure occurred inside dendritic structure. Mn and Si reduction with peak current increase it was observed, otherwise Ni content increase in samples with higher peak current, because of the base metal dilution increase.

PTA remelting process independently of the heat input used, promove an increase in HAZ length and microhardness if compared of ASP samples before remelting process.

5. ACKNOWLEDGMENTS

The authors thank the financial support of the Fundação Araucária, Institute of Technology for Development, LACTEC and Voight for the CA6NM used in this work.

6. REFERENCES

Akhtar A and Brodie N W, 1979, “Field-Welding Large Turbine Runners”. Water Power & Dam Construction, 40–46p.

Arai, Y.; Hikuchi, M.; Wtanabe, T.; Nakagaki, M., 1995, “Residual stress due to welding and its effect on the assessment of cracks near the weld interface. International Journal of Pressure Vessel and Piping”, No. 63, pp 237-248.

Bergeon, N., Guenin,G., Esnouf, C., 1997, “Characterization of the stress-induced o martensite in a Fe–Mn–Si–Cr–Ni shape memory alloy: microstructural observation at different scales, mechanism of formation and growth”. Materials Science and Engineering A, Vol. 238, No. 2, pp. 309–316.

Bilmes P.D., Llorente, C., Ipiña, J.P., 2000, “Toughness and Microstructure of 13Cr4NiMo High-Strength Steel Welds”. Journal of Materials Engineering and Performance, Vol. 9, number 6, 609–615p.

Bilmes, P. D.; Solari, M.; Llorente, C. L., 2001, “Characteristics and effects of austenite resulting from tempering of 13Cr-NiMo martensitic steel weld metals”. Materials Characterization, No. 46, pp.285–296.

Boy, J. H., Kumar, A., March, P., Willis, P., Herman, H., 1997, “Cavitation and Erosion Resistant Thermal Spray Coatings.” Construction Productivity Advancement Research [CPAR] Program. Technical Report 97/118.

Chiu, K.Y., Cheng, F.T., Man, H.C., 2005, “Laser cladding of austenitic stainless steel using NiTi strips for resisting cavitation erosion”. Materials Science and Engineering A, Vol. 402, No. 1-2, pp. 126-134.

Cui, Z.D., Man, H.C., Cheng, F.T., Yue, T.M., 2003, “Cavitation erosion–corrosion characteristics of laser surface modified NiTi shape memory alloy”, Surface & Coatings Technology, Vol. 162, No. 2-3, pp. 147–153.

Folkhard E, 1988, “Welding Metallurgy of Sainless Steels”, Springer- Verlag New York, 279 p.

Gireń, B.G., Szkodo, M., Steller J., 2005, “Cavitation erosion of some laser produced iron base corrosion resistant alloys”, Wear, Vo. 258, pp. 614-622.

Huth, Hans-Jörg, 2005, "Fatigue design of hydraulic turbine runners", Trodheim, Norway, Engineering Doctor Thesis, Department of Engineering Design and Materials, Norwegian University of Science and Technology, 178 p.

Kreye, H., Schwetzke, R., Buschinelli A., Boccanera, L., 1998, "Cavitation Erosion Resistant Coatings Produced by thermal Spraying and by Weld Cladding". Proceedings of the 15th International Thermal Spray Conference. Nice, France. May.

Kwok, C.T., Man, H.C., Cheng, F.T., 2001, "Cavitation erosion-corrosion behaviour of laser surface alloyed AISI 1050 mild steel using NiCrSiB", Materials Science and Engineering A, Vol. 303, pp. 250-261.

Lippold, J.C. and Kotecki, D., 2005, "Welding metallurgy and weldability of stainless steel", New Jersey: John Wiley & Sons, 2005, 357p.

March, Patrick, and Hubble, Jerry., 1996, "Evaluation of Relative Cavitation Erosion Rates For Base Materials, Weld Overlays, and Coatings". Report No. WR28-1-900-282, Tennessee Valley Authority Engineering Laboratory. Norris, TN.

Matsumura, O., Sumi, T., Tamura, N., Sakao, K., Furukawa, T., Otsuka, H., 2000, "Pseudoelasticity in an Fe-28Mn-6Si-5Cr shape memory alloy", Materials science and Engineering A, Vol. 279, pp. 201-206.

Mitelea, Ion et al., 2010, "Cavitation resistance coatings deposited on titanium alloys substrates by plasma spraying and electron beam remelting", METAL2010, International Conference on Metallurgy and Materials, Roznov pod Radhostem, Czech Republic.

Musardo, Gustavo Borges, et al., 2005, "Recuperação de turbinas hidráulicas cavitadas por deposição de revestimentos a base de cobalto – aspectos microestruturais", 60° Congresso da ABM , Associação Brasileira de Metalurgia, Materiais e Mineração, Belo Horizonte - MG, Brasil.

Newbery, A.,P., Grant, P.S., Neiser, R.A., 2005, "The velocity and temperature of steel droplets during eletric arc spraying", Surface & Coating Technology, Vol. 195, No. 1, pp. 91-101.

Newbery, A.P., Grant, P.S., 2006, "Oxidation during electric arc spray forming of steel", Journal of Materials Processing Technology, Vol. 178, No.1-3, pp.259-269.

Otsuka, H., Yamada, H., Maruyama, T., Tanahashi, H., Matsuda S., Murakami, M., 1990, "Effects of alloying aditions on Fe-Mn-Si Shape memory alloys", ISIJ International, Vol. 30, No. 8, pp. 674-679.

Pukasiewicz, A.G.M., 2008, "Desenvolvimento de revestimentos Fe-Mn-Cr-Si-Ni Resistentes à cavitação depositadas por aspersão ASP", Curitiba, Engineering Doctor Thesis, Departamento de Pós Graduação em Engenharia, Universidade Federal do Paraná, 173p.

Richman, R.H., e Mc´Naughton, W.P., 1990, "Correlation of Cavitation-Erosion Behavior with Mechanical Properties of Metals", Wear, Vol. 140, pp. 63-82

Simoneau, R.L.P., 1987, "Cavitation Erosion and Deformation Mechanism of Ni and Co Austenitic Stainless Steel", Proceedings of 7th Conference on Erosion by Liquid and Solid Impact, Cambridge, Inglaterra.

Simoneau, R.L.P., Vibratory, 1991, "Jet and Hydroturbine Cavitation Erosion", Cavitation and Multiphase Flow Forum, American Society of Mechanical Engineers.

Stella, J., Schüller, E., Heßing, C., Hamed, O.A., Pohl, M., Stöver D., 2006, "Cavitation erosion of plasma-sprayed NiTi coatings", Wear, Vol. 260, No. 9-10, pp. 1020-1027.

Wang, Z., Zhu, J., 2004, "Cavitation erosion of Fe-Mn-Si-Cr shape memory alloys", Wear, Vol. 256, No. 1-2, pp. 66-72.

Wang, Z., Zhu, J., 2003, "Effect of phase transformation on cavitation erosion resistance of some ferrous alloys", Materials Science and Engineering A, Vol. 358, No. 1-2, pp. 273-278.

5. RESPONSIBILITY NOTICE

The authors are the only responsible for the printed material included in this paper.